ORIGINAL RESEARCH

Age-Related Changes of Normal Cerebral and Cardiac Blood Flow in Children and Adults Aged 7 Months to 61 Years

Can Wu, MS; Amir R. Honarmand, MD; Susanne Schnell, PhD; Ryan Kuhn, BS; Samantha E. Schoeneman, BA; Sameer A. Ansari, MD, PhD; James Carr, MD; Michael Markl, PhD; Ali Shaibani, MD

***Background*—**Cerebral and cardiac blood flow are important to the pathophysiology and development of cerebro- and cardiovascular diseases. The purpose of this study was to investigate the age dependence of normal cerebral and cardiac hemodynamics in children and adults over a broad range of ages.

***Methods and Results*—**Overall, 52 children (aged 0.6–17.2 years) and 30 adults (aged 19.2–60.7 years) without cerebro- and cardiovascular diseases were included in this study. Intracranial 4-dimensional flow and cardiac 2-dimensional phase-contrast magnetic resonance imaging were performed for all participants to measure flow parameters in the major intracranial vessels and aorta. Total cerebral blood flow (TCBF), cardiac and cerebral indexes, brain volume, and global cerebral perfusion (TCBF/brain volume) were evaluated. Flow analysis revealed that TCBF increased significantly from age 7 months to 6 years ($P<0.001$) and declined thereafter ($P<0.001$). Both cardiac and cerebral indices declined with age ($P<0.001$). The ratio of TCBF to ascending aortic flow declined rapidly until age 18 years ($P<0.001$) and remained relatively stable thereafter. Age-related changes of cerebral vascular peak velocities exhibited a trend similar to TCBF. By comparison, aortic peak velocities maintained relatively high levels in children and declined with age in adults ($P<0.001$). TCBF significantly correlated with brain volume in adults ($P=0.005$) and in 2 pediatric subgroups, aged <7 years ($P<0.001$) and 7 to 18 years ($P=0.039$).

***Conclusions*—**Cerebral and cardiac flow parameters are highly associated with age. The findings collectively highlight the importance of age-matched control data for the characterization of intracranial and cardiac hemodynamics. **(*J Am Heart Assoc.* 2016;5:e002657 doi: 10.1161/JAHA.115.002657)**

Key Words: 4-dimensional flow • cardiac flow • cerebral blood flow • hemodynamics • magnetic resonance imaging

Cerebral and cardiac blood flow is essential to understanding the pathophysiology and development of cerebro- and cardiovascular diseases. Cerebrovascular diseases, such as cerebral arteriovenous malformations and intracranial vascular stenosis, are well known to cause abnormal cerebral blood flow in adults.[1,2] In children, cardiac and cerebral flow dynamics are also significantly affected by congenital heart diseases[3] and cerebrovascular diseases, such as Moyamoya disease,[4] cerebral venous sinus thrombosis,[5,6] and vein of Galen malformations.[7,8] Consequently, a good rationale exists for investigating normal flow across a broad range of ages, including children, for improved hemodynamic assessment in patients with these diseases.

A number of studies have shown that total cerebral blood flow (TCBF) and cardiac output (CO) are age-dependent[9–14]; however, the previous studies focused primarily on the determination of TCBF and CO in adult cohorts.[9–11,14] The association of TCBF and CO with age, particularly during early development in infants and children compared with adults, remains incompletely understood. Cardiac index is another clinically significant marker widely used for cardiac function assessment by correlating CO with a person's body surface area (BSA), which allows direct comparison of the cardiac function in large and small participants.[11] Cardiac index has been reported as a predictor of acute cardiac death in young children.[15] Recently, Jefferson et al reported that low cardiac index is associated with incident dementia and Alzheimer's disease.[16] Analogous to cardiac index, cerebral flow index

From the Department of Biomedical Engineering, McCormick School of Engineering, Northwestern University, Evanston, IL (C.W., M.M.); Departments of Radiology (C.W., A.R.H., S.S., S.A.A., J.C., M.M., A.S.), Neurological Surgery (S.A.A., A.S.), and Neurology (S.A.A.), Feinberg School of Medicine, Northwestern University, Chicago, IL; Department of Medical Imaging, Ann & Robert H. Lurie Children's Hospital of Chicago, IL (R.K., S.E.S., A.S.).

Correspondence to: Can Wu, MS, Departments of Biomedical Engineering and Radiology, Northwestern University, 737 N. Michigan Avenue, Suite 1600, Chicago, IL 60611. E-mail: canwu2016@u.northwestern.edu

Received October 5, 2015; accepted November 22, 2015.

(TCBF/BSA), as a novel flow marker, may provide new insight into the understanding of brain function. Nevertheless, the age dependence of cardiac and cerebral flow indexes are not well characterized, particularly in children. Furthermore, a systematic analysis of age-related changes in the fraction of cardiac outflow contributing to TCBF across a wide range of ages has not been performed.

Ultrasound-based techniques and 2-dimensional (2D) phase-contrast (PC) magnetic resonance imaging (MRI) have been used previously to measure cerebral and cardiac vascular flow and velocities.[9,11,12,17,18] Ultrasound measurements, however, are operator dependent and limited by an inadequate acoustic window when measuring blood flow in cerebral vessels distal to the circle of Willis. Moreover, 2D PC-MRI requires multiple scans with manual 2D plane placement perpendicular to the intracranial vessels of interest. In contrast, 4-dimensional (4D) flow MRI (time-resolved 3-dimensional [3D] PC-MRI) offers the advantage of full volumetric coverage of the cerebral vessels and enables retrospective flow quantification at any vessel position within the imaging volume.[19] Recently, 4D flow MRI has been reported to provide reliable flow assessment consistent with 2D PC-MRI for the measurement of pulsatile flow in cerebral arteries.[20–23]

The aim of this study was to systematically investigate the age-related changes of cerebral and cardiac flow using intracranial 4D flow and cardiac 2D PC-MRI and to establish age-specific reference values of the flow parameters across a broad range of ages spanning infancy to middle adulthood for improved hemodynamic assessment in patients with cardio- and cerebrovascular diseases.

Methods

Participants

This study included 52 children (21 female, age 7.9±5.0 years [range 0.6–17.2 years]) and 30 healthy adults (15 female, age 37.9±15.0 years [range 19.2–60.7 years]) (Table). All recruited participants were rigorously screened with medical history of cardio- and cerebrovascular problems, ECG, blood pressure, and other factors that may influence blood flow. Participants with any of the following conditions were excluded from the study: BSA >35 kg/m^2; blood pressure >160/90 mm Hg; and history of stroke, diabetes, cancer, liver or kidney disease, heart or brain surgery, arrhythmia, smoking, or drug abuse. The study was approved by the local institutional review board and conducted in accordance with the Health Insurance Portability and Accountability Act guidelines. Informed consent was obtained from all adult participants and from children's parents. In addition, adolescent assent was obtained for children aged 12 to 17 years.

Table. Participant Characteristics and Flow Parameters

	Age Groups		
	Child Volunteers (aged <18 years)	Adult Volunteers (aged 18–61 years)	*P* Values
Participant characteristics			
Number	52	30	
Mean age, y	7.9±5.0	37.9±15.0	
Age range, y	0.6 to 17.2	19.2 to 60.7	
Sex (male/female)	21/31	15/15	
Height, m	1.24±0.33	1.73±0.12	
Weight, kg	33.7±22.6	77.6±14.2	
Body surface area, m^2	1.05±0.49	1.92±0.23	
Body mass index, kg/m^2	19.29±4.65	25.95±3.58	
Heart rate, bpm	92.7±20.3	66.6±11.1	
Cerebral flow/structure parameters			
TCBF, mL/min	1101.6±258.0	700.2±113.4	<0.001
Cerebral flow index, L/min/m^2	1.32±0.67	0.37±0.08	<0.001
Brain volume, mL	1100.76±209.57	1189.67±99.34	0.032
Cerebral perfusion, mL/min/100 mL	102.35±26.98	58.89±8.28	<0.001
TCBF/AAo flow ratio (%)	32.7±12.8	14.5±2.6	<0.001
Cardiac flow parameters			
AAo flow, mL/min	3865.2±1426.2	4906.2±849.0	<0.001
DAo flow, mL/min	2007.0±1284.0	3231.6±688.2	<0.001
Cardiac index, L/min per m^2	3.98±0.82	2.58±0.52	<0.001
DAo/AAo flow ratio (%)	47.7±15.2	65.6±5.9	<0.001

Mean age, height, weight, body surface area, heart rate, and all flow parameters are presented as mean±SD. *P* values are calculated using 2-tailed *t* test ($P<0.05$ was considered statistically significant). AAo indicates ascending aorta; bpm, beats per minute; DAo, descending aorta; TCBF, total cerebral blood flow.

Magnetic Resonance Imaging

All MRI was performed on a 3- or 1.5-T MRI scanner (Magnetom Aera or Skyra; Siemens). Prior to flow imaging, standard T1-weighted sequences (in adults, magnetization-prepared rapid gradient-echo, or MPRAGE; in children: MPRAGE or fluid-attenuated inversion recovery, called FLAIR) were performed for brain volume calculation with the following parameters: T1-MPRAGE used repetition time 1900 ms, echo time 2.5 ms, field of view (180–250)×(224–250) mm^2, voxel size 1.0×1.0×1.0 mm^3, and flip angle 9°; T1-FLAIR used

repetition time 2000 ms, echo time 9 ms, inversion time 900 ms, echo train length 4, and voxel size $1.0\times1.0\times3.0$ mm^3. In addition, 3D axial time-of-flight magnetic resonance angiography was performed for setting up 4D flow imaging coverage. Intracranial 4D flow and cardiac 2D PC-MRI were performed in the same imaging session for all participants (Figure 1A). Children aged <6 years were scanned under anesthesia or sedation using inhalational anesthetic (sevoflurane, Ultane; Abbott Laboratories, Inc). All data were acquired during free breathing except the adult cardiac 2D PC-MRI data, which were acquired during a single breath hold.

Intracranial 4D flow imaging

The 4D flow imaging was performed with 3D volumetric coverage of the major cerebral vessels (Figure 1A) and 3-directional velocity encoding (V_x, V_y, and V_z); data acquisition was synchronized with prospective ECG gating. The following pulse-sequence parameters were used: repetition time 5.2 to 5.6 ms, echo time 2.8 to 3.2 ms, flip angle 15°, velocity sensitivity 80 cm/s (adults, children aged <4 years, and children aged >8 years) or 100 cm/s (children aged 4–8 years), field of view $(140–160)\times(180–220)$ mm^2, temporal resolution 41.6 to 44.8 ms, and voxel size $(1.1–1.2)\times(1.1–1.2)\times(1.2–1.4)$ mm^3; total acquisition time varied between 8 and 22 minutes depending on the heart rate of the participants during 4D flow imaging.

Cardiac 2D PC-MRI

Data were acquired with retrospective ECG gating and through-plane velocity encoding (V_z) at the level of the proximal ascending (AAo) and descending (DAo) aorta. Pulse sequence parameters were as follows: repetition time 6.7 to

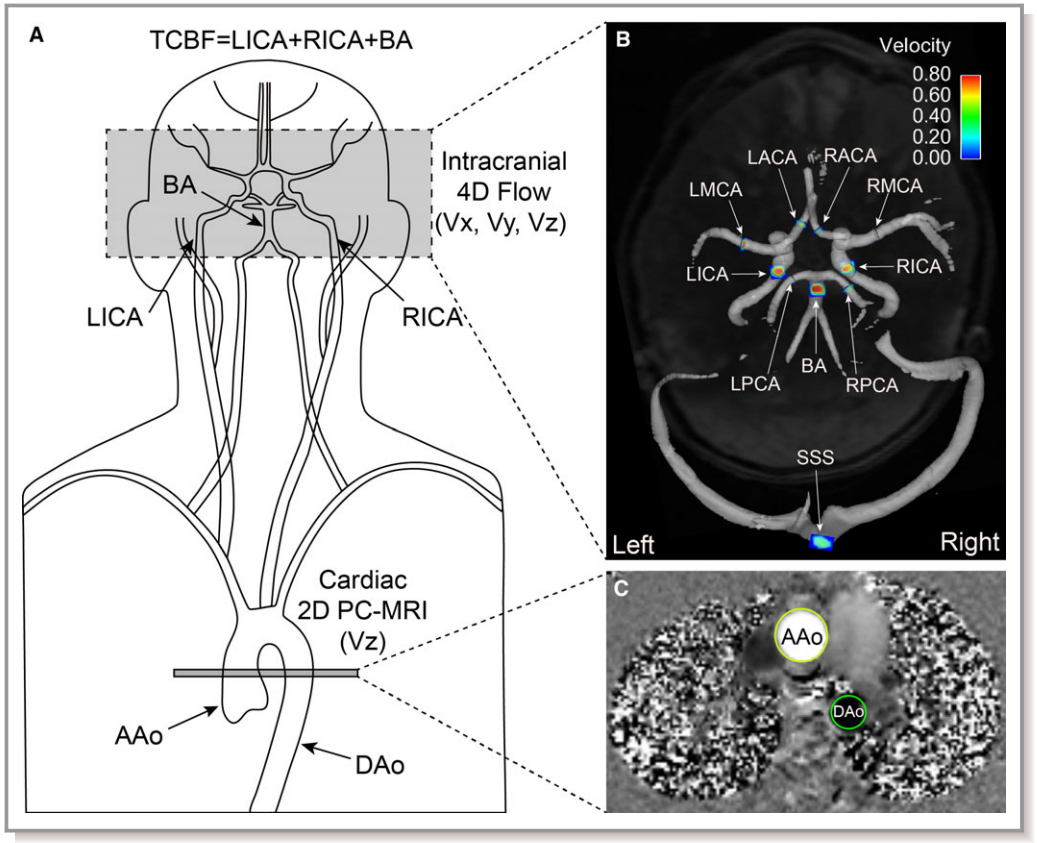

Figure 1. Schematic diagram illustrates the assessment of cerebrovascular blood flow using intracranial 4D flow MRI as well as the measurement of blood flow in the proximal AAo and DAo based on through-plane 2D time-resolved (CINE) PC-MRI (A). A 3-dimensional PC magnetic resonance angiogram was derived from the 4D flow data and used to define locations of 2D analysis planes for flow quantification in major intracranial vessels (B). 2D CINE PC-MRI image illustrates peak systolic blood flow in the aorta and vessel contours used for flow quantification in the AAo and DAo (C). 2D indicates 2-dimensional; 4D, 4-dimensional; AAo, ascending aorta; BA, basilar artery; DAo, descending aorta; LACA, left anterior cerebral artery; LICA, left internal carotid artery; LMCA, left middle cerebral artery; LPCA, left posterior cerebral artery; MRI, magnetic resonance imaging; PC, phase contrast; RACA, right anterior cerebral artery; RICA, right internal carotid artery; RMCA, right middle cerebral artery; RPCA, right posterior cerebral artery; SSS, superior sagittal sinus; TCBF, total cerebral blood flow; Vx,Vy,Vz, velocity encoding.

7.7 ms, echo time 2.4 to 2.9 ms, flip angle 30°, velocity sensitivity 150 cm/s, temporal resolution 26.8 to 30.8 ms, voxel size $1.2\times1.2\times7.0$ mm^3, and total acquisition time 12 to 22 seconds.

Flow Quantification

Cardiac flow quantification

Aortic flow parameters were evaluated with a combination of automatic propagation and manual adjustment of the AAo and DAo flow contours (Argus; Siemens) for all time frames over the cardiac cycle (example for a single time frame during systole shown in Figure 1C). Mean blood flow and peak velocities in the AAo and DAo were automatically calculated. In addition, cardiac index was calculated as the ratio of CO (CO equals AAo flow) and BSA: BSA $=\sqrt{\text{Weight}\times\text{Height}/3600}$.[24]

Cerebral flow quantification

All 4D flow data were preprocessed using an in-house tool in Matlab (MathWorks) to filter background noise and to correct for velocity aliasing and phase offset errors, as described previously.[25] In addition, a 3D PC magnetic resonance angiogram was calculated based on the absolute velocities weighted by the magnitude data.[19] The preprocessed data were imported into software (EnSight; CEI) for individual vascular flow quantification by using the previously calculated 3D PC magnetic resonance angiogram for anatomic orientation. The 2D analysis planes were manually positioned at predefined anatomic landmarks (Figure 1B): internal carotid arteries (ICAs; straight section between lacerum C3 and cavernous C4 segments), basilar artery (BA; middle portion between anterior inferior cerebellar artery and superior cerebellar artery), middle cerebral arteries (MCAs; middle M1 segment), anterior cerebral arteries (ACAs; middle A1 segment), posterior cerebral arteries (PCAs; middle P2 segment), and superior sagittal sinus (SSS; proximal to the confluence of sinuses). For each plane, mean blood flow over the cardiac cycle and peak velocities were automatically calculated. TCBF was calculated as cumulative flow in bilateral ICAs and BA.[26,27] Similar to cardiac index, cerebral flow index was calculated as the ratio of TCBF/BSA.

Correction for late diastolic flow

To minimize the effects of prospective ECG gating in 4D flow imaging on intracranial flow quantification, mean blood flow was corrected individually for each participant to include the missing late diastolic flow (often <10% of total flow) on the basis of the acquired flow profile and average heart rate (Figure 2). We hypothesized that blood flow at the beginning of the cardiac cycle would match the flow at end-diastole; therefore, the missing late diastolic flow

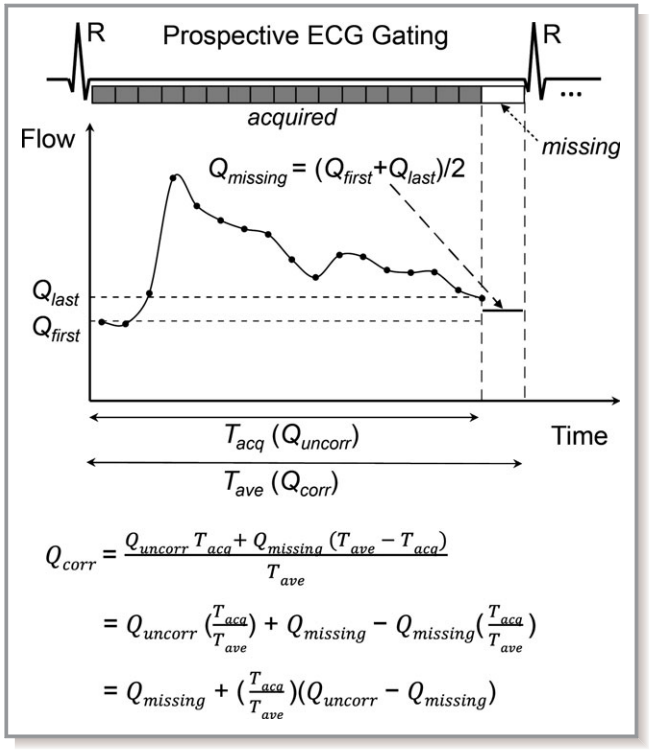

Figure 2. Correction for the mean intracranial blood flow to include the missing late diastole flow ($Q_{missing}$) based on the acquired flow profile and average heart rate (HR_{ave}) of each participant. Q_{first} and Q_{last} are the measured flow rates of the first and last time frames. Q_{corr} and Q_{uncorr} are mean blood flow before and after correction. T_{acq} and T_{ave} ($T_{ave}=60/HR_{ave}$) are the time intervals of the acquired flow profile and average time of the cardiac cycle, respectively.

($Q_{missing}=(Q_{first}+Q_{last})/2$) could be estimated as the average flow of the first (Q_{first}) and last (Q_{last}) time frame. The corrected mean flow was thus $Q_{corr}=Q_{missing}+(T_{acq}/T_{ave})\times(Q_{uncorr}-Q_{missing})$, in which Q_{uncorr} and Q_{corr} were mean flow before and after correction and T_{acq} and T_{ave} ($T_{ave}=60/$average heart rate) were the time intervals of the acquired flow profile and average time of the cardiac cycle, respectively.

Calculation of Brain Volume and Cerebral Perfusion

Brain volume was calculated from anatomic T1-weighted MRI using in-house automatic processing pipelines similar to the methods proposed by Ashburner and Friston.[28] Preprocessing steps and algorithms included coregistration, non–local means filtering, skull strip, and voxel-based morphometry. Segmentation of the white matter and gray matter was visually inspected and confirmed. Brain volume was calculated as the sum of white matter and gray matter volumes in milliliters. Global cerebral perfusion (mL/min per 100 mL) was then computed by dividing TCBF (mL/min) by brain volume (mL) and then multiplying by 100.[29]

Interobserver Reliability

A subset (10 children and 10 adults) of the study cohort was randomly chosen from each representative age group to evaluate the interobserver variability. Flow parameters (mean blood flow and peak velocity) in 3 representative intracranial vessels (ICAs and BA) and aorta (AAo and DAo) were measured by 2 experienced observers independently. Bland-Altman analysis (mean difference and 95% limits of agreement) and Lin's concordance correlation coefficient[30] (poor: $\rho_c<0.90$; moderate: $\rho_c\geq0.90$ to $\rho_c<0.95$; substantial: $\rho_c\geq0.95$ to $\rho_c\leq0.99$; almost perfect: $\rho_c>0.99$) were used to assess interobserver agreement. The 2 independent measurements were used for interobserver variability analysis, but all flow parameters presented in this study and used for further analysis were from a single observer.

Statistical Analysis

All cerebral and cardiac flow parameters were expressed as mean±SD. A Shapiro-Wilk test was used to determine the normality of the data distribution. Flow parameters in 2 different age/sex groups were compared using a 2-tailed *t* test (normal distribution) or a Mann–Whitney *U* test (nonnormal distribution). Cerebral and cardiac flow parameters (TCBF, aortic flow, cardiac index, cerebral flow index, TCBF/AAo flow ratio, DAo/AAo flow ratio, and peak velocities) in the male and female subgroups were separately plotted against age and fitted using linear, quadratic, or cubic polynomial regression. Note that the mean values of the peak velocities in the bilateral ICAs, ACAs, MCAs, and PCAs were used for the regression analysis. To highlight the fast changes of flow parameters during childhood, the age was scaled by one-fifth for adults aged >20 years. Relationships between 2 flow/structure parameters were assessed by Pearson's product moment correlation analysis, whereas associations between flow/structure parameters and age were evaluated by Spearman's rank correlation analysis (correlation coefficient *r* and *P* values were reported). All statistical analyses were performed using software package SPSS (version 20; IBM Corp) except Lin's concordance correlation coefficient, which was calculated using MedCalc (version 14.8.1; MedCalc Software). $P<0.05$ was considered statistically significant.

Results

Study Cohort

Participant demographics and characteristics are summarized in Table. A detailed distribution of age and sex for all participants is illustrated in Figure 3A. Intracranial and cardiac data were successfully acquired for all participants except for 2 children whose cardiac 2D PC-MRI data were not usable because of misplacement of the imaging slice. In addition, some cerebral vessels were not available for flow analysis because of vascular hypoplasia, slow flow, or insufficient imaging coverage. The number of cerebral vessels that could be used for flow analysis were as follows: ICAs (164 of 164, 100%), BA (82 of 82, 100%), ACAs (153 of 164, 93.3%), MCAs (158 of 164, 96.3%), PCAs (161 of 164, 98.2%), and SSS (79 of 82, 96.3%).

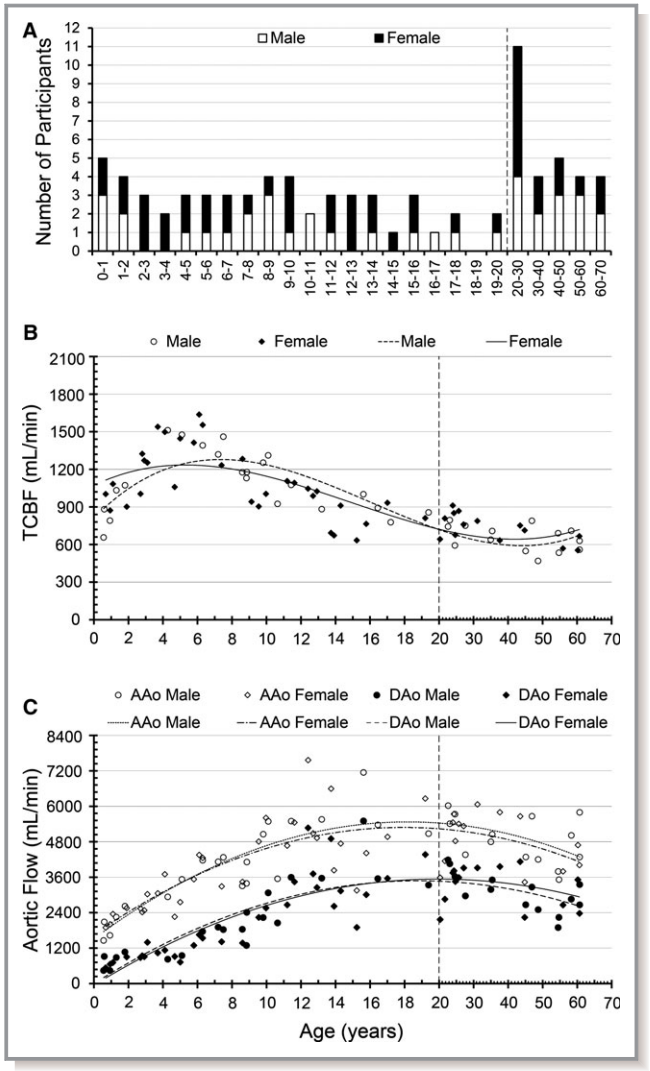

Figure 3. Age and sex distribution of the subjects included in this study (A). Age- and sex-related changes in TCBF (B) and aortic flow (C). TCBF and aortic flow are fitted using cubic and quadratic polynomial regression, respectively. Note that the horizontal axis (age) is scaled by one-fifth for adults aged >20 years for better appreciation of the fast flow changes in children. AAo indicates ascending aorta; DAo, descending aorta; TCBF, total cerebral blood flow.

Age-Related Changes in TCBF and Aortic Flow

A comparison of the cerebral (TCBF, cerebral flow index, brain volume, global cerebral perfusion, and TCBF/AAo flow ratio)

and cardiac (aortic flow, cardiac index, and DAo/AAo flow ratio) flow/structure parameters in children and adults are summarized in Table. All flow/structure parameters were significantly different between adults and children.

Cerebral flow was significantly associated with age (Figure 3B). Flow quantification demonstrated that TCBF increased rapidly from 7 months to 6 years of age at a rate of 120.6 mL/min per year (r=0.85, P<0.001), and declined thereafter until age 18 years at a slower rate of 51.6 mL/min per year (r=−0.76, P<0.001). TCBF continued to decline gradually in adults from age 18 to 61 years at a reduced rate of 4.8 mL/min per year (r=−0.63, P<0.001). TCBF was significantly higher in children compared with adults (1101.6±258.0 versus 700.2±113.4 mL/min, P<0.001).

In contrast to TCBF, AAo and DAo flow increased with age in children (aged <18 years) at a rate of 231.6 mL/min per year (r=0.81, P<0.001) and 222.0 mL/min per year (r=0.86, P<0.001), and declined thereafter until age 61 years at a slower rate of 22.8 mL/min per year (r=−0.40, P=0.027) and 24.0 mL/min per year (r=−0.52, P=0.003), respectively (Figure 3C). Both AAo (4906.2±849.0 versus 3865.2±1426.2 mL/min, P<0.001) and DAo flow (3231.6±688.2 versus 2007.0±1284.0 mL/min, P<0.001) in adults were significantly higher compared with children.

Age-Related Changes in Cardiac Index and Cerebral Flow Index

Cardiac index decreased with age in children (aged <18 years) at a rate of 0.11 L/min per m^2 per year (r=−0.65, P<0.001) and declined thereafter at a slower rate of 0.02 L/min per m^2 per year (r=−0.52, P=0.003) (Figure 4A). Similar to cardiac index, cerebral flow index decreased rapidly with age in children (aged <18 years) at a rate of 0.12 L/min per m^2 per year (r=−0.93, P<0.001) and continued to decline thereafter at a much slower rate of 0.003 L/min per m^2 per year (r=−0.61, P<0.001) (Figure 4B). Cerebral flow index significantly correlated with cardiac index (r=0.83, P<0.001).

TCBF/AAo and DAo/AAo Flow Ratios

TCBF/AAo flow ratio decreased rapidly from 45.5% in children aged <4 years to <20% in those aged 18 years (r=−0.90, P<0.001) and remained relatively stable thereafter (r=−0.17,

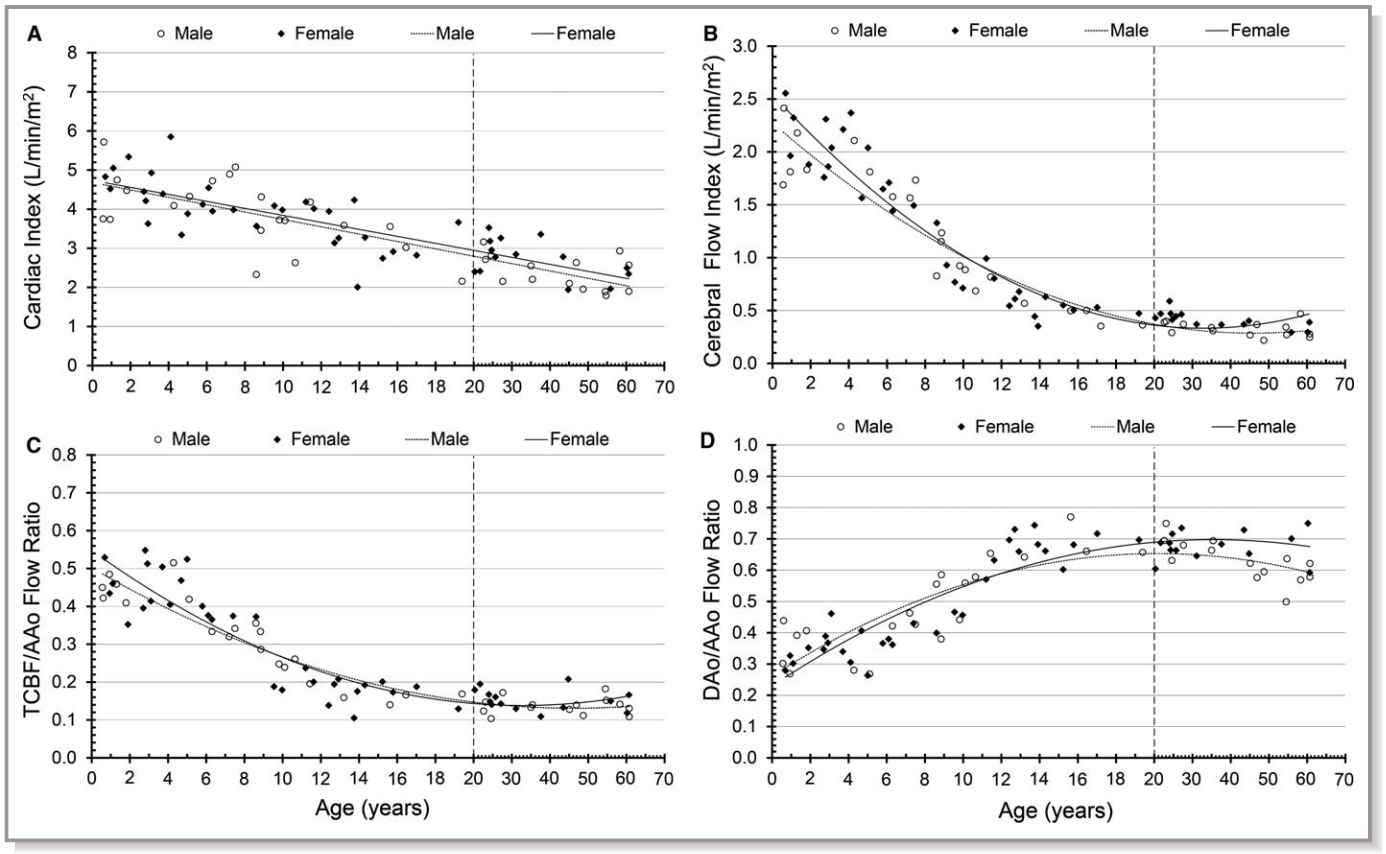

Figure 4. Age- and sex-related changes in cardiac index (A), cerebral flow index (B), TCBF to AAo flow ratio (C), and DAo to AAo flow ratio (D). Cardiac index was fitted using linear regression, whereas cerebral flow index, TCBF/AAo flow ratio, and DAo/AAo flow ratio were fitted using quadratic polynomial regression. AAo indicates ascending aorta; DAo, descending aorta; TCBF, total cerebral blood flow.

P=0.358) (Figure 4C). The average TCBF/AAo flow ratio in children was significantly higher compared with adults (32.7±12.8% versus 14.5±2.6%, P<0.001). In contrast to TCBF/AAo flow ratio, DAo/AAo flow ratio increased markedly from 35.5% in children aged <4 years to >60% in those aged 18 years (r=0.88, P<0.001) but declined slowly thereafter (r=−0.45, P=0.012) (Figure 4D). Average DAo/AAo flow ratio in children was significantly lower compared with adults (47.7±15.2% versus 65.6±5.9%, P<0.001).

Peak Velocities in Major Intracranial Vessels and Aorta

Age-related changes of peak velocities in the major intracranial vessels exhibited a trend similar to TCBF (shown in ICAs, BA, ACAs, MCAs, PCAs, and SSS) (Figure 5A through 5F). Cerebral vascular peak velocities increased rapidly from 7 months to ≈6 years of age and declined thereafter at a slower rate until age 18 years. The peak velocities in cerebral vessels continued to decline with age in adults except PCA and SSS (ICA: r=−0.71, P<0.001; BA: r=−0.51, P=0.004; ACA: r=−0.40, P=0.036; MCA: r=−0.42, P=0.044; PCA: r=−0.31, P=0.108; SSS: r=0.04, P=0.604).

Unlike a rapid increase of aortic flow in children (Figure 3C), peak velocities in the aorta maintained at relatively higher levels and were not significantly associated with age in children (AAo, 1.16±0.15 m/s, r=−0.04, P=0.796; DAo: 1.14±0.20 m/s, r=0.06, P=0.682) (Figure 5G and 5H). By comparison, peak velocities in the aorta declined with age in adults (AAo, 0.88±0.24 m/s, r=−0.73, P<0.001; DAo, 0.87±0.33 m/s, r=−0.74, P<0.001) (Figure 5G and 5H), which was in agreement with the declining aortic flow during this period (Figure 3C).

Brain Volume and Global Cerebral Perfusion

Brain volume increased with age in children (aged <18 years; r=0.72, P<0.001) and declined thereafter (r=−0.42, P=0.020) (Figure 6A). Global cerebral perfusion increased from 7 months to 4 years of age and declined thereafter until age 61 years (Figure 6B). TCBF significantly correlated with brain volume in adults (r=0.25, P=0.005) (Figure 6C). The correlation between TCBF and brain volume was not significant in children overall (r=0.18, P=0.205) (Figure 6C) but was significant in 2 child subgroups aged <7 years (r=0.82, P<0.001) and 7 to 18 years (r=0.39, P=0.039) (Figure 6D).

Sex-Related Differences in Flow/Structure Parameters

All cerebral and cardiac flow/structure parameters were not significantly different between sexes in children except for brain volume, which was higher in boys compared with girls (1179±232 versus 1050±179 mL, P=0.031). In contrast, cardiac index (P=0.023); cerebral flow index (P=0.001); DAo/AAo flow ratio (P=0.019); global cerebral perfusion (P=0.006); and peak velocities in the right MCA (P=0.037), SSS (P<0.001), and DAo (P=0.013) were significantly higher in female adults compared with male adults. All other cerebral and cardiac flow/structure parameters were not significantly different between male and female adults.

Interobserver Reliability

Bland-Altman analysis revealed good interobserver agreement with a low mean difference for blood flow and peak velocities in the intracranial arteries (ICAs and BA) and aorta (AAo and DAo). Mean difference for blood flow in the intracranial arteries and aorta were 1.2 mL/min (limits of agreement: −18.6 to 20.4 mL/min) and −15.6 mL/min (limits of agreement: −213.0 to 169.8 mL/min), respectively. Peak velocities in the intracranial arteries and aorta presented negligible interobserver difference in the intracranial arteries (mean difference −0.01 m/s, limits of agreement −0.05 to 0.04 m/s) and aorta (mean difference 0.00 m/s, limits of agreement −0.03 to 0.03 m/s). Lin's concordance correlation coefficient further confirmed excellent interobserver agreement (ρ_c=0.996 and ρ_c=0.991 for blood flow in intracranial arteries and aorta, respectively; ρ_c=0.996 and ρ_c=0.998 for peak velocities in intracranial arteries and aorta, respectively).

Discussion

In this study, age-specific and sex-related changes in normal cerebral and cardiac hemodynamics were evaluated in children and adult volunteers with a broad range of ages from 7 months to 61 years. We demonstrated that cerebral and cardiac flow parameters (eg, TCBF, cerebral flow index, cerebral perfusion, cardiac index, cerebral and aortic peak velocities) are highly associated with age, particularly during early childhood development. Maximum TCBF and cerebral artery peak velocities were reached at ≈6 years of age in children. The fraction of CO distributed to cerebral arteries (TCBF/AAo flow ratio) declined rapidly after 4 years of age and remained relatively stable during adulthood. In addition, significant correlation between TCBF and brain volume was identified in adults and 2 child subgroups.

To our knowledge, the impact of age, particularly during early childhood, on cerebral blood flow accounting for cardiac outflow has not been reported previously. We demonstrated that the TCBF/AAo flow ratio declined rapidly after 4 years of age in children. Although the absolute values of cerebral and

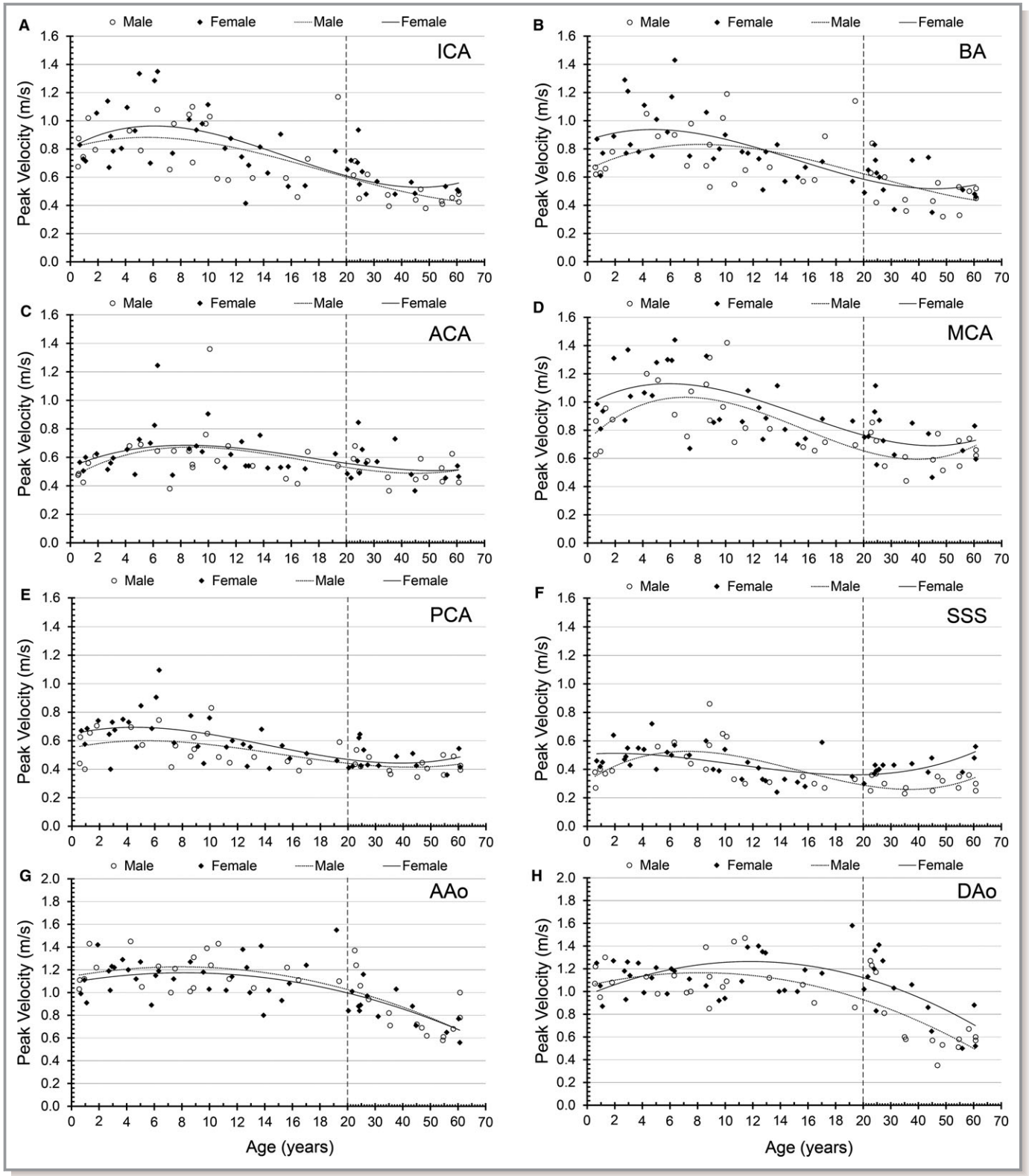

Figure 5. Age- and sex-related changes of peak velocities in the major intracranial vessels and aorta: ICA (A), BA (B), ACA (C), MCA (D), PCA (E), SSS (F), AAo (G) and DAo (H). Cerebral vascular peak velocities (A through F) were fitted using cubic polynomial regression, whereas aortic peak velocities (G and H) were fitted using quadratic polynomial regression. AAo indicates ascending aorta; ACA, anterior cerebral artery; BA, basilar artery; DAo, descending aorta; ICA, internal carotid artery; MCA, middle cerebral artery; PCA, posterior cerebral artery; SSS, superior sagittal sinus.

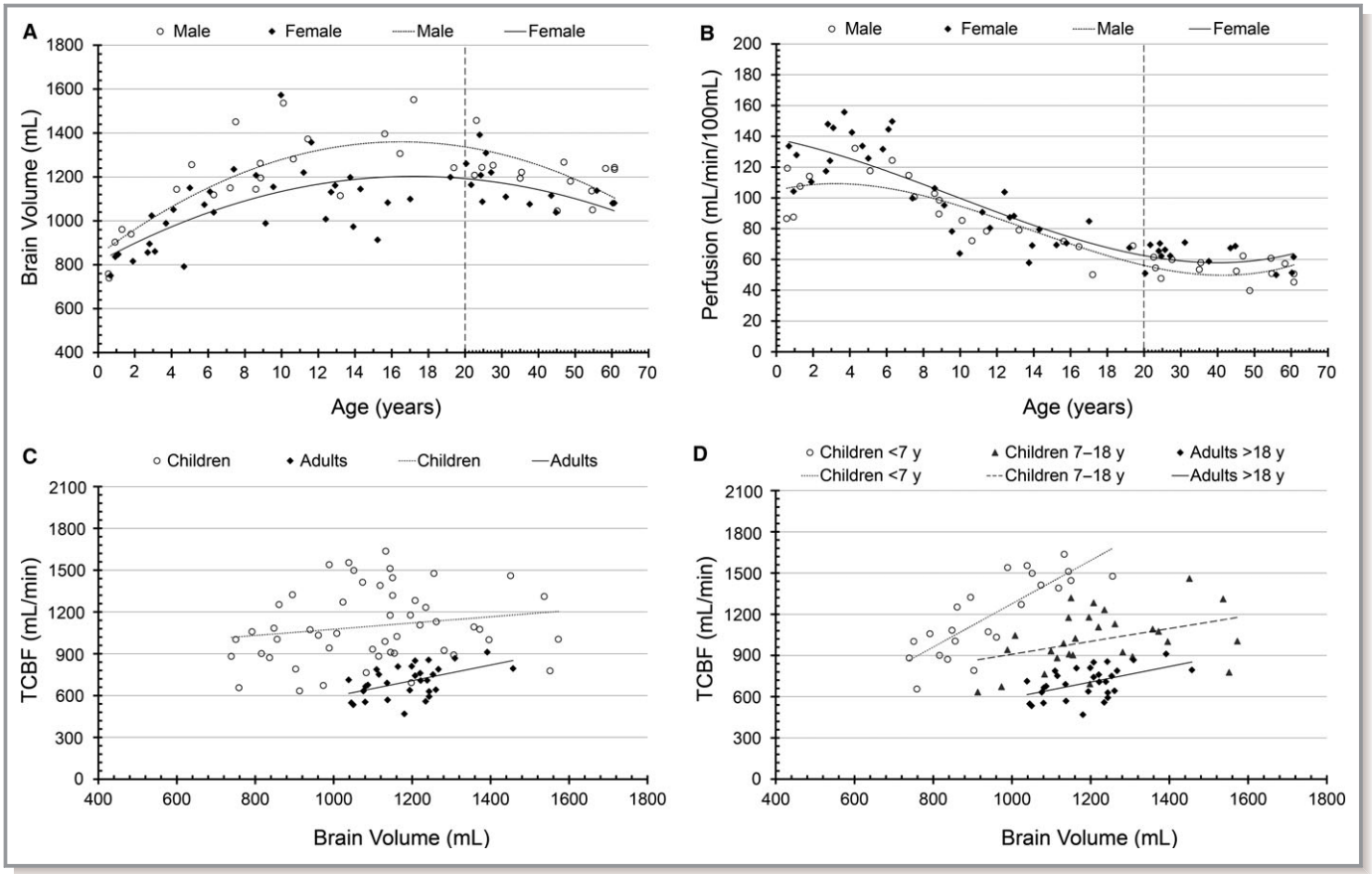

Figure 6. Age- and sex-related changes in brain volume (A) and global cerebral perfusion (B) correlation of TCBF and brain volume in children and adults (C), and correlation of TCBF and brain volume in adults and 2 child subgroups aged <7 years and 7 to 18 years (D). Brain volume and global cerebral perfusion were fitted using quadratic and cubic polynomial regression, respectively. TCBF indicates total cerebral blood flow.

cardiac flow declined significantly with age in adults ($P<0.001$), decrease in the fraction of CO to the brain was not significant throughout adulthood ($P=0.358$). The average TCBF/AAo flow ratio in adults was 14.5±2.6%, which agrees with previous studies showing that the TCBF fraction of the CO was between 10% to 16% in adults based on different measurement methods (eg, nitrous oxide, MRI, and video dilution techniques).[31–33] In addition, the average DAo/AAo flow ratio in the adult cohort (aged 38±15 years [range 19–61 years]) was 65.6±5.9%, which was comparable to the previously reported value of 64±8% in 12 age-matched healthy adults (aged 37±15 years [range 18–62 years]).[34]

Previous studies reported abnormal cerebral blood flow in adult patients with cerebrovascular diseases, such as cerebral artery stenosis and arteriovenous malformations.[1,2,35] In addition, global brain hypoperfusion (ie, low total cerebral arterial inflow) has been demonstrated to be a potential risk factor for development and progression of mild cognitive impairment and Alzheimer's disease in elderly participants.[36,37] Cerebral flow dynamics has also been shown to be greatly affected in children with various cerebral vascular disorders. Moyamoya disease is a major cause of ischemic stroke in children, and cerebral blood flow was found to be significantly lower in children with Moyamoya disease compared with age-matched healthy participants.[4] Cerebral venous sinus thrombosis is another pathology that may result in decreased cerebral blood flow, possibly due to increased venous pressure.[5,6] Vein of Galen malformation is a congenital cerebrovascular disease that primarily affects infants and young children and has been shown to cause abnormal cardiac and cerebral flow.[7,8] Sickle cell disease has also been shown to be associated with abnormal cerebral blood flow and velocities in children.[38,39] In addition, congenital heart disease has a significant impact on cerebral blood flow and brain development as a result of flow disturbances from cardiac abnormality.[3] Consequently, determination of normal values of cerebral and cardiac flow parameters, particularly considering the effects of age, can be of significant benefit in treatment planning and outcome evaluation in the management of these diseases.

Few studies have investigated TCBF in children with a broad range of ages comparable to our pediatric study cohort. An early study by Schoning et al investigated the age dependence of TCBF in 94 children aged 3 to 18 years, using

a computed sonography system.[13] The study demonstrated that TCBF increased significantly from ages 3 to 6.5 years and declined thereafter to a relatively constant level at age 15 years. Another study, by Bode et al, demonstrated that the maximum systolic peak flow velocity in the basal cerebral arteries was reached around age 6 years by investigating 112 healthy children aged between 1 day and 18 years, using transcranial Doppler sonography.[40] In our study, we applied in vivo intracranial 4D flow imaging and demonstrated that the age for maximum TCBF and systolic peak flow velocities in the basal cerebral arteries was between 5 and 7 years, which agrees well with the previous findings derived from ultrasound-based techniques.

Schoning et al also demonstrated that average TCBF was 760±129 and 781±112 mL/min for girls and boys, respectively.[13] In contrast, Lin et al reported much higher TCBF of 1538±416 mL/min in a group of preschool children aged 4 to 6 years.[18] In our study, the average TCBF of 1101±258 mL/min in children was in between the previously reported values. Discrepancies in participant selection (eg, age distribution), prescribed vessel locations, and imaging techniques (sonography versus MRI) can be potential factors accounting for the high variability of TCBF in children. The measured TCBF in 30 healthy adults was 700±113 mL/min, which was also within the range of previously reported TCBF varying from 492 to 768 mL/min.[9,12–14,26,27,41] In addition, our study revealed that TCBF declined at a rate of 4.2 mL/min per year in adults, comparable to the findings of previous studies with an annual decrease of TCBF between 2.6 and 4.8 mL/min.[9,26,42,43]

Significant differences in most flow parameters were observed between children and adults (Table), highlighting the importance of age-matched control data for hemodynamic evaluation in the cardiovascular system. The brain is one of the most metabolically active organs in the body. Significantly higher TCBF in children indicates higher cerebral metabolic rate and thus elevated physiochemical activity compared with adults. CO (AAo flow), the volume of blood delivered to the body, is an important indicator of cardiac function. DAo flow supplies the key organs in the lower body, such as liver, kidney, spleen, and intestine. Significantly higher AAo and DAo flow in adults is consistent with the higher demand of blood to the body related to increased body size in comparison with children. Cardiac and cerebral flow indexes were normalized to each participant's BSA, providing flow measures independent of body size. Significantly higher flow indexes in children suggest higher averaged metabolic rate. We also noted that the fraction of CO delivered to the brain (TCBF/AAo flow ratio) in children was more than twice of the fraction in adults. This finding indicates a higher proportion of blood supply to the brain and thus increased cerebral oxygen consumption in children compared with adults.

TCBF can be measured as a summation of blood flow in bilateral ICAs and vertebral arteries (ie, cervical blood flow)[9,13,14,36] or in bilateral ICAs and BA (ie, cerebral blood flow).[26,27,42,43] We calculated TCBF using the latter method for 2 reasons. First, relatively long acquisition time for 4D flow MRI limits the imaging volume to cover the vertebral arteries. The other reason lies in the fact that the vertebral arteries are typically smaller compared with the BA and usually asymmetric, thus measuring blood flow in the BA instead of vertebral arteries can potentially minimize partial volume effects. In addition, no significant difference was identified between mean cervical and cerebral blood flow in healthy adults.[44]

TCBF was significantly correlated with brain volume in adults (P=0.005), similar to the findings from a recent study that reported a linear relationship (P<0.001) between TCBF and brain volume in 49 healthy adults.[29] In addition, we identified significant correlation between TCBF and brain volume in 2 pediatric subgroups aged <7 years (P<0.001) and 7 to 18 years (P=0.039). These findings indicated that brain volume is a strong determinant of cerebral blood flow.

Global cerebral perfusion reached its maximum in children aged between 3 and 4 years, characterized by 2.7 times as much cerebral perfusion at this stage as that of adults. Similar to our findings, Wintermark et al reported peak cerebral perfusion at 2 to 4 years of age, with global average cerebral perfusion exceeding that of adults by a factor of 2.5.[45]

It has been well documented that cardiac index declines with age in adults.[10,11] We confirmed the decrease of cardiac index at a rate of 18 mL/min per m^2 per year in adults, similar to the decrease of 23 mL/min per m^2 per year reported by Katori[46] The association of cerebral flow index in children and adults with a broad range of ages has not been reported. Similar to cardiac index, we identified that cerebral flow index declined rapidly with age in children (aged <18 years) and continued to decline at a much slower rate in adults. In addition, we observed significant correlation between cerebral flow index and cardiac index, indicating that cerebral flow index as a novel marker together with cardiac index may provide new insight into the understanding of brain function and autoregulatory mechanisms for maintaining cerebral blood flow.

The influence of sex on cardiac and cerebral blood flow is not well established, particularly in childhood. Some studies reported significant sex differences in TCBF,[14,27] whereas other studies did not identify sex-specific changes in flow.[9,12,13] In our study, no significant difference in TCBF was observed between sexes for both healthy children and adults. The sex difference in blood flow velocities in the cerebral vessels is also controversial. Some studies have demonstrated higher cerebral vascular flow velocities in female participants compared with male participants,[47,48] whereas others reported no sex-related difference.[49,50] We observed no significant differences of peak velocities in

cerebral vessels except the right MCA and SSS, which were significantly higher in female adults. In contrast to the previous findings, which showed that cardiac index did not differ between male and female adult participants,[11,17] we observed significantly higher cardiac index (also cerebral flow index) in female adults compared with male adults related to significantly lower BSA in women. The discrepancy of sex differences in flow parameters may arise from different participant cohorts and imaging techniques.

It remains controversial how anesthesia (sedation) can affect cardiac and cerebral blood flow in terms of anesthetic type, dosage, and anesthesia duration. Some studies reported dose-dependent decrease in CO and cerebral blood flow possibly due to lowered requirements of oxygen for tissue metabolism,[51,52] whereas others revealed no significant change or increase of cardiac and cerebral blood flow.[53–55] The influence of sevoflurane, an anesthetic used in this study, on cardiac and cerebral blood flow is also controversial, including reports of decreased, unchanged, and increased blood flow.[56–61] Further studies including pre- and postanesthesia scans are warranted to investigate the impact of anesthetics on both cardiac and cerebral flow dynamics.

Although different field strengths (1.5 and 3 T) were used for MRI scans, depending on the availability of the scanners, the influence of different field strengths on blood flow measurements was minor because previous studies reported no significant difference of flow quantification in cerebral vessels and the thoracic aorta between 1.5 and 3 T MRI.[62,63]

To take advantages of 3D volume coverage and short scan time, 4D flow and 2D PC-MRI were used for measuring cerebral and cardiac flow, respectively. The effect of mixed use of 4D flow and 2D PC-MRI should be considered when characterizing the fraction of CO distributed to cerebral arteries (ie, TCBF/AAo flow ratio). Previous studies have shown that 4D flow MRI provided flow measurements comparable to 2D PC-MRI in cerebral and cardiac systems.[20,22,64,65] Consequently, the influence of mixing 2D and 4D PC-MRI on the assessment of cerebral and cardiac flow was expected to be minor.

Limitations

Our study has some limitations. Partial volume effects have previously been reported to significantly affect the accuracy of PC-MRI flow quantification for the voxel size exceeding one-third of the vessel diameter.[66] In our study, we used an in-plane resolution of 1.1 to 1.2 mm, which should not cause severe partial volume effects for TCBF measurement, considering the normal diameters of the ICAs (mean: 4.3±0.5 mm) and BA (mean: 3.82±0.47 mm).[67,68] The resolution, however, was not optimal to estimate mean blood flow in the smaller distal arteries of the Circle of Willis, particularly in the ACAs (2.8±0.4 mm) and PCAs (2.2±0.6 mm).[67,69] In addition, smaller cerebral vessel diameters in early childhood presented an additional challenge when attempting to accurately quantify cerebral vascular blood flow. Furthermore, the impact of partial volume effects is potentially inhomogeneous among different age ranges because the size of the cerebral vessels is age dependent. Consequently, the age-appropriate cerebral and cardiac flow values presented in this study may not be definitive but strongly underscore the importance of age-matched flow studies. A number of methods have been proposed to correct for partial volume errors.[70–72] Further studies are warranted to investigate these methods in combination with 4D flow MRI for improved flow measurement in smaller cerebral vessels.

The 4D flow sequence used in this study allowed only a single velocity sensitivity value that was prescribed before the scan. Notably, velocity aliasing was observed in some of the children and young adults, particularly in the MCAs, which typically carry the highest blood flow velocity in the brain. Velocity aliasing was successfully corrected during data preprocessing and thus had no effect on flow quantification. It is appropriate to set the velocity sensitivity value of 100 cm/s for children aged between 4 and 8 years and 80 cm/s for adults and children aged <4 or >8 years, considering that the peak velocities in the MCAs were 0.98±0.26 and 0.71±0.17 m/s for children and adults, respectively, and reached the maximum at ≈6 years of age. Nevertheless, the venous flow measurement may be compromised because of a lower velocity/contrast ratio in the venous system. Advanced 4D flow imaging with dual or variable velocity encoding strategies is promising for improved cerebral flow quantification.[73,74]

Another limitation of the 4D flow technique used in this study is its inability to capture the blood flow in the entire cardiac cycle with prospective ECG gating. Although a direct comparison of the flow parameters between prospective and retrospective ECG-gated imaging was not available, we attempted to minimize the effects of prospective ECG gating on cerebral blood flow quantification by correcting the end-diastolic flow. The cardiac lengths are highly variable among the age ranges of the participants—typically, young children have a shorter cardiac cycle (higher heart rate) than that of adults—however, the correction of missing end-diastolic flow was performed individually for each participant based on the averaged cardiac cycle length (RR interval) specific to the participant during the 4D flow scan. Consequently, the influence of variant cardiac lengths on end-diastolic flow correction among different age ranges was minor. The missing end-diastolic length accounted for the total cardiac cycle was 15.7±8.9% and 16.8±6.9% for children and adults, respectively; however, the difference in TCBF before and after end-diastolic flow correction was only 5.3±4.9% and

5.5±2.4% for children and adults, respectively, which further confirmed that flow correction was independent of heart rate. Considering the pulsatile feature of blood flow in cerebral arteries, it is appropriate to use prospective ECG-gated 4D flow imaging in combination with end-diastolic flow correction for cerebral flow assessment in participants of various ages (heart rates).

Conclusions

This study demonstrates that cerebral and cardiac hemodynamics can be assessed simultaneously using in vivo 4D flow and 2D PC-MRI, respectively. The data provide age-specific changes of normal cerebral and cardiac blood flow parameters in a cohort of children and adults covering a broad range of ages. The findings collectively highlight the importance of age-matched control data in the evaluation of cerebral and cardiac hemodynamics and provide additional insight into the understanding of normal brain development in relation to cardiac physiology, particularly in children.

Sources of Funding

Grant support by American Heart Association (AHA) Predoctoral Fellowship 14PRE18370014, Radiological Society of North America (RSNA) Research Seed Grant RSD1207, and SIR Foundation Pilot Research Grant.

Disclosures

None.

References

1. Meinel FG, Fischer J, Pomschar A, Wohrle N, Koerte IK, Steffinger D, Laubender RP, Muacevic A, Reiser MF, Alperin N, Ertl-Wagner B. MRI evidence for preserved regulation of intracranial pressure in patients with cerebral arteriovenous malformations. *Eur J Radiol*. 2014;83:1442–1447.
2. Neff KW, Horn P, Schmiedek P, Duber C, Dinter DJ. 2D Cine phase-contrast MRI for volume flow evaluation of the brain-supplying circulation in moyamoya disease. *AJR Am J Roentgenol*. 2006;187:W107–W115.
3. Donofrio MT, Massaro AN. Impact of congenital heart disease on brain development and neurodevelopmental outcome. *Int J Pediatr*. 2010;2010:359390, doi:10.1155/2010/359390.
4. Ogawa A, Yoshimoto T, Suzuki J, Sakurai Y. Cerebral blood flow in moyamoya disease. Part 1: correlation with age and regional distribution. *Acta Neurochir (Wien)*. 1990;105:30–34.
5. Hashmi M, Wasay M. Caring for cerebral venous sinus thrombosis in children. *J Emerg Trauma Shock*. 2011;4:389–394.
6. Sebire G, Tabarki B, Saunders DE, Leroy I, Liesner R, Saint-Martin C, Husson B, Williams AN, Wade A, Kirkham FJ. Cerebral venous sinus thrombosis in children: risk factors, presentation, diagnosis and outcome. *Brain*. 2005;128:477–489.
7. Patel N, Mills JF, Cheung MM, Loughnan PM. Systemic haemodynamics in infants with vein of Galen malformation: assessment and basis for therapy. *J Perinatol*. 2007;27:460–463.
8. Rizzo G, Arduini D, Colosimo C Jr, Boccolini MR, Mancuso S. Abnormal fetal cerebral blood flow velocity waveforms as a sign of an aneurysm of the vein of Galen. *Fetal Ther*. 1987;2:75–79.
9. Amin-Hanjani S, Du X, Pandey DK, Thulborn KR, Charbel FT. Effect of age and vascular anatomy on blood flow in major cerebral vessels. *J Cereb Blood Flow Metab*. 2015;35:312–318.
10. Brandfonbrener M, Landowne M, Shock NW. Changes in cardiac output with age. *Circulation*. 1955;12:557–566.
11. Carlsson M, Andersson R, Bloch KM, Steding-Ehrenborg K, Mosen H, Stahlberg F, Ekmehag B, Arheden H. Cardiac output and cardiac index measured with cardiovascular magnetic resonance in healthy subjects, elite athletes and patients with congestive heart failure. *J Cardiovasc Magn Reson*. 2012;14:51.
12. Scheel P, Ruge C, Petruch UR, Schoning M. Color duplex measurement of cerebral blood flow volume in healthy adults. *Stroke*. 2000;31:147–150.
13. Schoning M, Hartig B. Age dependence of total cerebral blood flow volume from childhood to adulthood. *J Cereb Blood Flow Metab*. 1996;16:827–833.
14. Tarumi T, Ayaz Khan M, Liu J, Tseng BY, Parker R, Riley J, Tinajero C, Zhang R. Cerebral hemodynamics in normal aging: central artery stiffness, wave reflection, and pressure pulsatility. *J Cereb Blood Flow Metab*. 2014;34:971–978.
15. Parr GV, Blackstone EH, Kirklin JW. Cardiac performance and mortality early after intracardiac surgery in infants and young children. *Circulation*. 1975;51:867–874.
16. Jefferson AL, Beiser AS, Himali JJ, Seshadri S, O'Donnell CJ, Manning WJ, Wolf PA, Au R, Benjamin EJ. Low cardiac index is associated with incident dementia and Alzheimer disease the Framingham Heart Study. *Circulation*. 2015;131:1333–1339.
17. Collis T, Devereux RB, Roman MJ, de Simone G, Yeh J, Howard BV, Fabsitz RR, Welty TK. Relations of stroke volume and cardiac output to body composition: the Strong Heart Study. *Circulation*. 2001;103:820–825.
18. Lin KL, Chen KS, Hsieh MY, Wang HS. Transcranial color Doppler sonography on healthy pre-school children: flow velocities and total cerebral blood flow volume. *Brain Dev*. 2007;29:64–68.
19. Markl M, Frydrychowicz A, Kozerke S, Hope M, Wieben O. 4D Flow MRI. *J Magn Reson Imaging*. 2012;36:1015–1036.
20. Wahlin A, Ambarki K, Birgander R, Wieben O, Johnson KM, Malm J, Eklund A. Measuring pulsatile flow in cerebral arteries using 4D phase-contrast MR imaging. *AJNR Am J Neuroradiol*. 2013;34:1740–1745.
21. Chang W, Landgraf B, Johnson KM, Kecskemeti S, Wu Y, Velikina J, Rowley H, Wieben O, Mistretta C, Turski P. Velocity measurements in the middle cerebral arteries of healthy volunteers using 3D radial phase-contrast HYPRFlow: comparison with transcranial Doppler sonography and 2D phase-contrast MR imaging. *AJNR Am J Neuroradiol*. 2011;32:54–59.
22. Gu T, Korosec FR, Block WF, Fain SB, Turk Q, Lum D, Zhou Y, Grist TM, Haughton V, Mistretta CA. PC VIPR: a high-speed 3D phase-contrast method for flow quantification and high-resolution angiography. *AJNR Am J Neuroradiol*. 2005;26:743–749.
23. Meckel S, Leitner L, Bonati LH, Santini F, Schubert T, Stalder AF, Lyrer P, Markl M, Wetzel SG. Intracranial artery velocity measurement using 4D PC MRI at 3 T: comparison with transcranial ultrasound techniques and 2D PC MRI. *Neuroradiology*. 2013;55:389–398.
24. Mosteller RD. Simplified calculation of body-surface area. *N Engl J Med*. 1987;317:1098.
25. Bock J, Kreher BW, Hennig J, Markl M. Optimized pre-processing of time-resolved 2D and 3D phase contrast MRI data. In Proceedings: 15th Scientific Meeting of the International Society for Magnetic Resonance in Medicine. 2007:3138.
26. Buijs PC, Krabbe-Hartkamp MJ, Bakker CJ, de Lange EE, Ramos LM, Breteler MM, Mali WP. Effect of age on cerebral blood flow: measurement with ungated two-dimensional phase-contrast MR angiography in 250 adults. *Radiology*. 1998;209:667–674.
27. Vernooij MW, van der Lugt A, Ikram MA, Wielopolski PA, Vrooman HA, Hofman A, Krestin GP, Breteler MM. Total cerebral blood flow and total brain perfusion in the general population: the Rotterdam Scan Study. *J Cereb Blood Flow Metab*. 2008;28:412–419.
28. Ashburner J, Friston KJ. Voxel-based morphometry–the methods. *Neuroimage*. 2000;11:805–821.
29. Zarrinkoob L, Ambarki K, Wahlin A, Birgander R, Eklund A, Malm J. Blood flow distribution in cerebral arteries. *J Cereb Blood Flow Metab*. 2015;35:648–654.
30. Lin LI. A concordance correlation coefficient to evaluate reproducibility. *Biometrics*. 1989;45:255–268.
31. Henriksen OM, Jensen LT, Krabbe K, Larsson HBW, Rostrup E. Relationship between cardiac function and resting cerebral blood flow: MRI measurements in healthy elderly subjects. *Clin Physiol Funct Imaging*. 2014;34:471–477.
32. Lantz BM, Foerster JM, Link DP, Holcroft JW. Regional distribution of cardiac output: normal values in man determined by video dilution technique. *AJR Am J Roentgenol*. 1981;137:903–907.

33. Williams LR, Leggett RW. Reference values for resting blood flow to organs of man. *Clin Phys Physiol Meas*. 1989;10:187–217.
34. Mohiaddin RH, Kilner PJ, Rees S, Longmore DB. Magnetic resonance volume flow and jet velocity mapping in aortic coarctation. *J Am Coll Cardiol*. 1993;22:1515–1521.
35. Wu C, Ansari SA, Honarmand AR, Vakil P, Hurley MC, Bendok BR, Carr J, Carroll TJ, Markl M. Evaluation of 4D vascular flow and tissue perfusion in cerebral arteriovenous malformations: influence of Spetzler-Martin grade, clinical presentation, and AVM risk factors. *AJNR Am J Neuroradiol*. 2015;36:1142–1149.
36. Liu J, Zhu YS, Khan MA, Brunk E, Martin-Cook K, Weiner MF, Cullum CM, Lu H, Levine BD, Diaz-Arrastia R, Zhang R. Global brain hypoperfusion and oxygenation in amnestic mild cognitive impairment. *Alzheimers Dement*. 2014;10:162–170.
37. Ruitenberg A, den Heijer T, Bakker SL, van Swieten JC, Koudstaal PJ, Hofman A, Breteler MM. Cerebral hypoperfusion and clinical onset of dementia: the Rotterdam Study. *Ann Neurol*. 2005;57:789–794.
38. Arkuszewski M, Krejza J, Chen R, Kwiatkowski JL, Ichord R, Zimmerman R, Ohene-Frempong K, Desiderio L, Melhem ER. Sickle cell disease: reference values and interhemispheric differences of nonimaging transcranial Doppler blood flow parameters. *AJNR Am J Neuroradiol*. 2011;32:1444–1450.
39. Behpour AM, Shah PS, Mikulis DJ, Kassner A. Cerebral blood flow abnormalities in children with sickle cell disease: a systematic review. *Pediatr Neurol*. 2013;48:188–199.
40. Bode H, Wais U. Age dependence of flow velocities in basal cerebral arteries. *Arch Dis Child*. 1988;63:606–611.
41. Spilt A, Van den Boom R, Kamper AM, Blauw GJ, Bollen EL, van Buchem MA. MR assessment of cerebral vascular response: a comparison of two methods. *J Magn Reson Imaging*. 2002;16:610–616.
42. Hendrikse J, van Raamt AF, van der Graaf Y, Mali WP, van der Grond J. Distribution of cerebral blood flow in the circle of Willis. *Radiology*. 2005;235:184–189.
43. van Raamt AF, Appelman AP, Mali WP, van der Graaf Y; Group SS. Arterial blood flow to the brain in patients with vascular disease: the SMART Study. *Radiology*. 2006;240:515–521.
44. Stoquart-Elsankari S, Lehmann P, Villette A, Czosnyka M, Meyer ME, Deramond H, Baledent O. A phase-contrast MRI study of physiologic cerebral venous flow. *J Cereb Blood Flow Metab*. 2009;29:1208–1215.
45. Wintermark M, Lepori D, Cotting J, Roulet E, van Melle G, Meuli R, Maeder P, Regli L, Verdun FR, Deonna T, Schnyder P, Gudinchet F. Brain perfusion in children: evolution with age assessed by quantitative perfusion computed tomography. *Pediatrics*. 2004;113:1642–1652.
46. Katori R. Normal cardiac output in relation to age and body size. *Tohoku J Exp Med*. 1979;128:377–387.
47. Albayrak R, Degirmenci B, Acar M, Haktanir A, Colbay M, Yaman M. Doppler sonography evaluation of flow velocity and volume of the extracranial internal carotid and vertebral arteries in healthy adults. *J Clin Ultrasound*. 2007;35:27–33.
48. Vavilala MS, Kincaid MS, Muangman SL, Suz P, Rozet I, Lam AM. Gender differences in cerebral blood flow velocity and autoregulation between the anterior and posterior circulations in healthy children. *Pediatr Res*. 2005;58:574–578.
49. Scheel P, Ruge C, Schoning M. Flow velocity and flow volume measurements in the extracranial carotid and vertebral arteries in healthy adults: reference data and the effects of age. *Ultrasound Med Biol*. 2000;26:1261–1266.
50. Torbey MT, Hauser TK, Bhardwaj A, Williams MA, Ulatowski JA, Mirski MA, Razumovsky AY. Effect of age on cerebral blood flow velocity and incidence of vasospasm after aneurysmal subarachnoid hemorrhage. *Stroke*. 2001;32:2005–2011.
51. Goodchild CS, Serrao JM. Cardiovascular effects of propofol in the anaesthetized dog. *Br J Anaesth*. 1989;63:87–92.
52. Van Aken H, Van Hemelrijck J. Influence of anesthesia on cerebral blood flow and cerebral metabolism: an overview. *Agressologie*. 1991;32:303–306.
53. Mayberg TS, Lam AM, Matta BF, Domino KB, Winn HR. Ketamine does not increase cerebral blood-flow velocity or intracranial-pressure during isoflurane nitrous-oxide anesthesia in patients undergoing craniotomy. *Anest Analg*. 1995;81:84–89.
54. Raux O, Rochette A, Morau E, Dadure C, Vergnes C, Capdevila X. The effects of spread of block and adrenaline on cardiac output after epidural anesthesia in young children: a randomized, double-blind, prospective study. *Anesth Analg*. 2004;98:948–955.
55. Vajramuni GV, Umamaheswara Rao GS, Pillai SV. Cerebral blood flow velocity changes under nitrous oxide halothane anesthesia in patients with frontotemporal gliomas: a comparison of the normal and abnormal cerebral hemispheres. *Neurol India*. 2004;52:79–81.
56. Bundgaard H, von Oettingen G, Larsen KM, Landsfeldt U, Jensen KA, Nielsen E, Cold GE. Effects of sevoflurane on intracranial pressure, cerebral blood flow and cerebral metabolism. A dose-response study in patients subjected to craniotomy for cerebral tumours. *Acta Anaesthesiol Scand*. 1998;42:621–627.
57. Kawana S, Wachi J, Nakayama M, Namiki A. Comparison of haemodynamic changes induced by sevoflurane and halothane in paediatric patients. *Can J Anaesth*. 1995;42:603–607.
58. Oshima T, Karasawa F, Okazaki Y, Wada H, Satoh T. Effects of sevoflurane on cerebral blood flow and cerebral metabolic rate of oxygen in human beings: a comparison with isoflurane. *Eur J Anaesthesiol*. 2003;20:543–547.
59. Reinsfelt B, Westerlind A, Ricksten SE. The effects of sevoflurane on cerebral blood flow autoregulation and flow-metabolism coupling during cardiopulmonary bypass. *Acta Anaesthesiol Scand*. 2011;55:118–123.
60. Scheller MS, Nakakimura K, Fleischer JE, Zornow MH. Cerebral effects of sevoflurane in the dog: comparison with isoflurane and enflurane. *Br J Anaesth*. 1990;65:388–392.
61. Wodey E, Pladys P, Copin C, Lucas MM, Chaumont A, Carre P, Lelong B, Azzis O, Ecoffey C. Comparative hemodynamic depression of sevoflurane versus halothane in infants: an echocardiographic study. *Anesthesiology*. 1997;87:795–800.
62. Bammer R, Hope TA, Aksoy M, Alley MT. Time-resolved 3D quantitative flow MRI of the major intracranial vessels: initial experience and comparative evaluation at 1.5T and 3.0T in combination with parallel imaging. *Magn Reson Med*. 2007;57:127–140.
63. Strecker C, Harloff A, Wallis W, Markl M. Flow-sensitive 4D MRI of the thoracic aorta: comparison of image quality, quantitative flow, and wall parameters at 1.5 T and 3 T. *J Magn Reson Imaging*. 2012;36:1097–1103.
64. Gabbour M, Schnell S, Jarvis K, Robinson JD, Markl M, Rigsby CK. 4-D Flow magnetic resonance imaging: blood flow quantification compared to 2-D phase-contrast magnetic resonance imaging and Doppler echocardiography. *Pediatr Radiol*. 2015;45:804–813.
65. Nordmeyer S, Riesenkampff E, Crelier G, Khasheei A, Schnackenburg B, Berger F, Kuehne T. Flow-sensitive four-dimensional cine magnetic resonance imaging for offline blood flow quantification in multiple vessels: a validation study. *J Magn Reson Imaging*. 2010;32:677–683.
66. Lotz J, Meier C, Leppert A, Galanski M. Cardiovascular flow measurement with phase-contrast MR imaging: basic facts and implementation. *Radiographics*. 2002;22:651–671.
67. Muller HR, Brunholzl C, Radu EW, Buser M. Sex and side differences of cerebral arterial caliber. *Neuroradiology*. 1991;33:212–216.
68. Zhang DP, Zhang SL, Zhang JW, Zhang HT, Fu SQ, Yu M, Ren YF, Ji P. Basilar artery bending length, vascular risk factors, and pontine infarction. *J Neurol Sci*. 2014;338:142–147.
69. Kamath S. Observations on the length and diameter of vessels forming the circle of Willis. *J Anat*. 1981;133:419–423.
70. Hoogeveen RM, Bakker CJ, Viergever MA. MR phase-contrast flow measurement with limited spatial resolution in small vessels: value of model-based image analysis. *Magn Reson Med*. 1999;41:520–528.
71. Lagerstrand KM, Lehmann H, Starck G, Vikhoff-Baaz B, Ekholm S, Forssell-Aronsson E. Method to correct for the effects of limited spatial resolution in phase-contrast flow MRI measurements. *Magn Reson Med*. 2002;48:883–889.
72. Tang C, Blatter DD, Parker DL. Correction of partial-volume effects in phase-contrast flow measurements. *J Magn Reson Imaging*. 1995;5:175–180.
73. Nett EJ, Johnson KM, Frydrychowicz A, Del Rio AM, Schrauben E, Francois CJ, Wieben O. Four-dimensional phase contrast MRI with accelerated dual velocity encoding. *J Magn Reson Imaging*. 2012;35:1462–1471.
74. Nilsson A, Bloch KM, Carlsson M, Heiberg E, Stahlberg F. Variable velocity encoding in a three-dimensional, three-directional phase contrast sequence: evaluation in phantom and volunteers. *J Magn Reson Imaging*. 2012;36:1450–1459.